

**PHOTOCATALYTIC SEAWATER  
DESALINATION: THE EFFECT OF METAL  
LOADING IN THE HYBRID  $\text{TiO}_2$  AND THE  
EFFECT OF WAVELENGTH**

**AFIQ HAFIZI BIN AZIZI**

Thesis submitted in partial fulfilment of the requirements  
for the award of the degree of  
Bachelor of Chemical Engineering

**Faculty of Chemical & Natural Resources Engineering  
UNIVERSITI MALAYSIA PAHANG**

JULY 2015

©AFIQ HAFIZI BIN AZIZI (2015)

## ABSTRACT

Hybrid photocatalyst of Titanium Dioxide ( $\text{TiO}_2$ ) and biomass ash catalyst become an attractive alternative promoter for seawater desalination. The effect of metal loading in the seawater desalination via photocatalytic reaction at different wavelength light source was investigated. The hybrid catalyst with different weight ratio of  $\text{TiO}_2$ , Oil palm fiber ash and metal loading either Nickel or Ferum was synthesized via wet impregnation. The catalysts were then characterized by using Scanning Electron Microscopy (SEM), Brunauer Emmett Teller (BET), X-ray Diffraction (XRD). The natural seawater were analysed for its pH, conductivity, turbidity, Biochemical Oxygen Demand (BOD) and Chemical Oxygen Demand (COD) prior the experiment. Then the catalyst was tested with the natural seawater using photocatalytic reactor with the weight ratio of 1:400 catalyst and seawater. The experiment was conducted for two hours in a mercury light exposure with the wavelength of 365 nm and 420 nm respectively. The pH, conductivity, turbidity, BOD and COD of the final product were analysed. It is found that there was an increment of the seawater quality in term of salt concentration, COD and BOD. By using 365 nm wavelength light and nickel loading catalyst, the salt concentration, COD and BOD reduced up to 4%, 88%, and 68% respectively. Meanwhile, the reduction of COD and BOD were achieved at 95% and 97% when 420 nm wavelength light and ferum loading catalyst were used. At 420 nm wave length, the salt concentration was increasing due to the distillation. It because at 420 nm wavelength the water was heated up to 100 °C and causing the distillation to dominates the process. Nickel loading catalyst perform at best when 365 nm light was used, while ferum loading work great when 420 nm light was used. It is because the performance of the metal loading was due to the different characterization of the metal band gap in which the smaller the band gap, the bigger the wavelength. Nickel has bigger band gap than ferum. It can be concluded that the addition of the metal loading improve the performance of the catalyst due to the different band characterization of the metal loading and changes of wavelength can affect the performance of the catalyst.

## **ABSTRAK**

Fotomangkin hibrid Titanium Dioksida ( $\text{TiO}_2$ ) dan pemangkin abu biomas menjadi promoter alternatif menarik bagi penyahmasinan air laut. Kesan pembebanan logam di penyahgaraman air laut melalui reaksi fotopemangkinan pada sumber cahaya yang berbeza panjang gelombang dikaji. Pemangkin hibrid dengan nisbah yang berbeza berat  $\text{TiO}_2$ , abu serat kelapa sawit dan muatan logam sama ada Nikel atau Ferum telah disintesis melalui pengisitepuan basah. Pemangkin kemudian dicirikan dengan menggunakan Scanning Electron Microscopy (SEM), Brunauer Emmett Teller (BET), X-ray Diffraction (XRD). Air laut semula jadi dianalisis untuk yang pH, kekonduksian, kekeruhan, Keperluan Oksigen Biokimia (BOD) dan Permintaan Oksigen Kimia (COD) sebelum percubaan. Kemudian pemangkin diuji dengan air laut yang semula jadi dengan menggunakan reaktor fotopemangkinan dengan nisbah berat 1: 400 pemangkin dan air laut. Eksperimen ini dijalankan selama dua jam dalam pendedahan cahaya merkuri dengan panjang gelombang 365 nm dan 420 nm masing-masing. pH, kekonduksian, kekeruhan, BOD dan COD produk akhir telah dianalisis. Didapati bahawa terdapat peningkatan kualiti air laut dari segi kepekatan garam, COD dan BOD. Dengan menggunakan 365 nm panjang gelombang cahaya dan nikel mangkin, kepekatan garam, COD dan BOD dikurangkan sehingga masing-masing kepada 4 %, 88 %, dan 68 %. Sementara itu, pengurangan COD dan BOD telah dicapai pada 95 % dan 97 % apabila 420 nm cahaya panjang gelombang dan ferum mangkin digunakan. Pada 420 nm panjang gelombang, kepekatan garam yang semakin meningkat disebabkan oleh penyulingan. Ia kerana pada 420 nm panjang gelombang, air telah dipanaskan sehingga 100 °C dan menyebabkan penyulingan untuk menguasai proses. Nikel loading prestasi terbaik apabila 365 nm cahaya telah digunakan, manakala prestasi terbaik ferum loading apabila 420 nm cahaya telah digunakan. Ia adalah kerana prestasi loading besi ini bergantung pada perwatakan yang berbeza daripada jurang jalur logam di mana lebih kecil jurang ini, semakin besar panjang gelombang. Nikel mempunyai jurang jalur lebih besar daripada ferum. Ia boleh membuat kesimpulan bahawa penambahan muatan logam meningkatkan prestasi pemangkin kerana pencirian yang berbeza muatan logam dan perubahan panjang gelombang boleh mengubah prestasi pemangkin.

# TABLE OF CONTENTS

|   |      |
|---|------|
| SUPERVISOR'S DECLARATION .....  | V    |
| STUDENT'S DECLARATION .....   | VI   |
| <i>Dedication</i> .....   | VII  |
| ACKNOWLEDGEMENT .....   | VIII |
| ABSTRACT.....   | IX   |
| ABSTRAK.....  | X    |
| TABLE OF CONTENTS.....  | XI   |
| LIST OF FIGURES .....   | XIII |
| LIST OF TABLES .....  | XV   |
| LIST OF ABBREVIATIONS.....  | XVI  |
| 1 INTRODUCTION.....   | 1    |
| 1.1 Research Background .....   | 1    |
| 1.2 Motivation and statement of problem .....   | 2    |
| 1.3 Objectives.....   | 4    |
| 1.4 Scope of this research .....  | 4    |
| 2 LITERATURE REVIEW .....   | 5    |
| 2.1 Introduction.....   | 5    |
| 2.2 Photocatalytic process.....   | 5    |
| 2.3 Photocatalytic Reactor .....  | 6    |
| 2.4 Titanium Dioxide (TiO <sub>2</sub> ).....   | 7    |
| 2.5 Mechanism of Photocatalytic Reaction.....   | 7    |
| 2.6 Oil palm fiber ash (Biomass Ash).....   | 9    |
| 2.7 Metal Loading in Photocatalyst .....  | 10   |
| 3 MATERIALS AND METHODS .....   | 11   |
| 3.1 Introduction.....   | 11   |
| 3.2 Material .....  | 12   |
| 3.2.1 Natural Seawater (NSW).....   | 12   |
| The NSW sample from Teluk Cempedak Kuantan, Pahang. The sample was stored at 4 °C in the refrigerator. .... | 12   |
| 3.2.2 Oil palm fiber ash (Biomass ash) .....  | 12   |
| 3.2.3 Chemical.....   | 12   |
| 3.3 Preparation of Solution and Catalyst .....  | 12   |
| 3.3.1 Preparation of NSW .....  | 12   |
| 3.3.2 Preparation of Catalyst .....   | 13   |
| 3.3.3 Characterization of Catalyst .....  | 13   |
| 3.4 Photocatalytic Reactor Set Up .....   | 15   |
| 3.5 Experimental Procedure.....   | 16   |
| 3.6 Analytical Test .....   | 16   |
| 3.6.1 pH, Conductivity and Total Dissolved Solid (TDS) .....  | 16   |
| 3.6.2 Chemical Oxygen Demand (COD) .....  | 17   |
| 3.6.3 Biochemical Oxygen Demand (BOD) .....   | 18   |
| 4 RESULT AND DISCUSSION.....  | 19   |
| 4.1 Introduction.....   | 19   |
| 4.2 Property of Seawater Sample.....  | 19   |
| 4.3 The Effect of Metal Loading.....  | 20   |

|       |                                     |    |
|-------|-------------------------------------|----|
| 4.4   | The Effect of Wavelength .....      | 27 |
| 4.4.1 | No Metal Loading .....              | 28 |
| 4.4.2 | Nickel Loading .....                | 34 |
| 4.4.3 | Ferum Loading .....                 | 40 |
| 4.4.4 | SEM Characterization .....          | 46 |
| 4.4.5 | Summary .....                       | 47 |
| 5     | CONCLUSION AND RECOMMENDATION ..... | 49 |
| 5.1   | Conclusion .....                    | 49 |
| 5.2   | Recommendation .....                | 50 |
|       | References.....                     | 51 |
|       | APPENDICES .....                    | 55 |

## LIST OF FIGURES

|  |    |
|--|----|
| Figure 3-1: Flow diagram of experimental procedure. ....   | 11 |
| Figure 3-2: Scanning Electron Microscopy (SEM). ....   | 14 |
| Figure 3-3: Brunauer Emmett Teller (BET). ....   | 14 |
| Figure 3-4: X-Ray Diffraction (XRD). ....  | 15 |
| Figure 3-5: The schematic diagram of photocatalytic reactor .....  | 15 |
| Figure 3-6: pH, conductivity and TDS meter. ....   | 17 |
| Figure 3-7: COD measuring equipment (a) COD digestion reactor (b) COD<br>spectrophotometer.....  | 17 |
| Figure 3-8: Dissolved oxygen meter.....  | 18 |
| Figure 4-1: SEM image of the fresh catalyst: a) no metal b) with nickel loading c) with<br>ferum loading.....  | 20 |
| Figure 4-2: Percentage of reduction for the NSW analysis. ....   | 21 |
| Figure 4-3: Percentage of reduction for the conductivity of NSW analysis. ....   | 22 |
| Figure 4-4: Percentage of reduction for the TDS of NSW analysis. ....  | 23 |
| Figure 4-5: XRD analysis for the metal loading catalyst.....   | 23 |
| Figure 4-6: Percentage of reduction for the BOD of NSW analysis. ....  | 25 |
| Figure 4-7: Percentage of reduction for the COD of NSW analysis. ....  | 26 |
| Figure 4-8: SEM image of the used catalyst: (a) fresh no metal loading (b) used no<br>metal loading (c)fresh nickel loading (d) used nickel loading (e) fresh ferum loading<br>(f) used ferum loading..... | 27 |
| Figure 4-9: NSW analysis for pH. ....  | 29 |
| Figure 4-10: Percentage of reduction for pH. ....  | 29 |
| Figure 4-11: NSW analysis for conductivity. ....   | 30 |
| Figure 4-12: NSW analysis for TDS.....   | 30 |
| Figure 4-13: XRD analysis (a) 365 nm (b) 420 nm.....   | 31 |
| Figure 4-14: NSW analysis for BOD.....   | 32 |
| Figure 4-15: Percentage of reduction for BOD. ....   | 33 |
| Figure 4-16: NSW analysis for COD.....   | 33 |
| Figure 4-17: Percentage of reduction for COD. ....   | 34 |
| Figure 4-18: NSW analysis for pH. ....   | 35 |
| Figure 4-19: Percentage of reduction for pH. ....  | 35 |
| Figure 4-20: NSW analysis for conductivity. ....   | 36 |
| Figure 4-21: NSW analysis for TDS.....   | 36 |
| Figure 4-22: XRD analysis (a) 365 nm (b) 420 nm.....   | 37 |

|   |    |
|---|----|
| Figure 4-23: NSW analysis for BOD.....  | 38 |
| Figure 4-24: Percentage of reduction for BOD. ....  | 39 |
| Figure 4-25: NSW analysis for COD.....  | 39 |
| Figure 4-26: Percentage of reduction for COD. ....  | 40 |
| Figure 4-27: NSW analysis for pH. ....  | 41 |
| Figure 4-28: NSW analysis for conductivity. ....  | 42 |
| Figure 4-29: NSW analysis for TDS.....  | 42 |
| Figure 4-30: XRD analysis (a) 365 nm (b) 420 nm.....  | 43 |
| Figure 4-31: NSW analysis for BOD.....  | 44 |
| Figure 4-32: Percentage of reduction for BOD. ....  | 45 |
| Figure 4-33: NSW analysis for COD.....  | 45 |
| Figure 4-34: Percentage of reduction for COD. ....  | 46 |
| Figure 4-35: SEM image of the used catalyst: (a) fresh no metal loading (b) used no metal loading (c)fresh nickel loading (d) used nickel loading (e) fresh ferum loading (f) used ferum loading..... | 47 |
| Figure 4-36 : The overall comparison for the percentage of reduction for 365 nm and 420 nm wavelength light.....  | 48 |

## LIST OF TABLES

|   |    |
|---|----|
| Table 2-1: General mechanism of the photocatalytic reaction on illuminated TiO <sub>2</sub> (Teh & Mohamed 2011)..... | 8  |
| Table 2-2: The research on utilization of fly ash.....  | 9  |
| Table 2-3: The research on effect of metal in photocatalyst.....  | 10 |
| Table 3-1: The weight ratio of the three catalyst.....  | 13 |
| Table 4-1: Fresh NSW analysis .....   | 19 |
| Table 4-2: NSW analysis after the photocatalytic reaction.....  | 21 |
| Table 4-3: BET analysis for the metal loading catalyst.....   | 24 |
| Table 4-4: NSW analysis after the photocatalytic reaction at 420 nm.....  | 28 |
| Table 4-5: NSW analysis for no metal loading catalyst.....  | 28 |
| Table 4-6: BET analysis for no metal loading catalyst.....  | 31 |
| Table 4-7: NSW analysis for nickel loading catalyst.....  | 34 |
| Table 4-8: BET analysis for no metal loading catalyst.....  | 37 |
| Table 4-9: NSW analysis for nickel loading catalyst.....  | 41 |
| Table 4-10: BET analysis for ferum loading catalyst.....  | 43 |

## LIST OF ABBREVIATIONS

|  |                              |
|--|------------------------------|
| TiO <sub>2</sub>                                       | Titanium dioxide             |
| COD  | Chemical Oxygen Demand       |
| BOD  | Biochemical Oxygen Demand    |
| SEM  | Scanning Electron Microscopy |
| BET  | Brunnauer Emmett Teller      |
| XRD  | X-ray Diffraction            |
| NSW  | Natural seawater             |
| (Ni(NO <sub>3</sub> ) <sub>2</sub> ·6H <sub>2</sub> O) | Nickel Nitrate Hexahydrate   |
| (Fe(NO <sub>3</sub> ) <sub>3</sub> ·9H <sub>2</sub> O) | Ferum Nitrate Hydrate        |
| VB   | Valence band                 |
| CB   | Conduction band              |
| E <sub>bg</sub>  | Band gap energy              |

# 1 INTRODUCTION

## 1.1 Research Background

Water is made out of two hydrogen and one oxygen, it is one of the most essential elements to health and is so important that your body actually has a specific drought management system in place to prevent dehydration and ensure your survival. Water makes up more than two thirds of human body weight, and without water, we would die in a few days. The human brain is made up of 95 % water, blood is 82 % and lungs 90 %. A mere 2 % drop in our body's water supply can trigger signs of dehydration: fuzzy short-term memory, trouble with basic math, and difficulty focusing on smaller print, such as a computer screen. Therefore water is essential to sustain the human life and good clean water accessibility is very importance. These is because good access to clean water will benefit us with good health and prevent hydration of the body. The problem faced nowadays is the water shortag (Shakhashiri, 2011)e problem due to the expanding of world population and the current water source is fresh water where it only covered 1.7 % of the world water. Therefore seawater which cover 96 % of the world water has to use (Wolf, 1999). The country that has started to u (Esplugas, et al., 2002) (Pera-Titus, et al., 2004)se seawater as their main source of water are the Middle East country and Africa. Both country depend on the desalinate seawater to overcome their water shortage problem (Ghaffour, et al., 2011).

The seawater can be desalinate to clean water using several method like distillation (Ghaffour, et al., 2011)where the water is heated at high temperature so that the water evaporates and separated from the salt, electrodialysis where the salt ion is transport from one solution through ion-exchange membranes to another solution under the influence of an applied electric potential difference, and the reverse osmosis (Akili, et al., 2008) (Francois, et al., 2008) method where membrane is used. The method used for desalination of seawater mostly require high energy which will lead to high cost (Shakhashiri, 2011). That is why there still many country that have not use seawater as their main source of water supplies even though seawater cover 96 % of the world water.

The researcher nowadays also, are trying to develop or modified the current technologies for seawater desalination so that the energy and cost consumption can be reduced.

These have led to the study in the field of advanced oxidation process (AOP) as the alternative to the desalination technologies. The rationales of these AOPs are based on the in-situ generation of highly reactive transitory species for mineralization of refractory organic compounds, water pathogens and disinfection by-products (Esplugas, et al., 2002) (Pera-Titus, et al., 2004). Among these AOPs, heterogeneous photocatalysis employing semiconductor catalysts ( $\text{TiO}_2$ ,  $\text{ZnO}$ ,  $\text{Fe}_2\text{O}_3$ ,  $\text{CdS}$ ,  $\text{GaP}$  and  $\text{ZnS}$ ) has demonstrated its efficiency in degrading a wide range of ambiguous refractory organics into readily biodegradable compounds, and eventually mineralized them to innocuous carbon dioxide and water. Among the semiconductor catalysts, titanium dioxide ( $\text{TiO}_2$ ) has received the greatest interest. The  $\text{TiO}_2$  is the most active photocatalyst under the photon energy of  $300 \text{ nm} < \lambda < 390 \text{ nm}$  and remains stable after the repeated catalytic cycles, whereas  $\text{CdS}$  or  $\text{GaP}$  are degraded along to produce toxic products (Malato, et al., 2009). Other than these, the multi-faceted functional properties of  $\text{TiO}_2$  catalyst, such as their chemical and thermal stability or resistance to chemical breakdown and their strong mechanical properties have promoted its wide application in photocatalytic water treatment (Chong, 2010).

For these study, the photocatalytic reaction of the Titanium Dioxide was tested on the seawater in order to see the effectiveness of the reaction to absorb the salt content of the seawater and purification of the seawater. In these study also the Titanium Dioxide was mixed with biomass ash and metal as supported catalyst in order to improve the efficiency and the performance of the catalyst. The catalyst also was tested with different wavelength to see whether the performance of the catalyst increase or decrease due to the different wavelength light.

## **1.2 Motivation and statement of problem**

Water is known as a colourless, transparent, odourless, liquid which forms the seas, lakes, rivers and rain and is the basis fluid of the living organism (Anon., 2014). All form of life need water and human consume drinking water which has qualities with the human body. Ordinary rain water in many countries has been polluted and therefore it is not safe to

drink directly. This natural resource has become scarce with the growing world population, and its availability is a major social and economic concern (Anon., 2004).

Based on the U.S Geological Survey, it is found that 96.5% Earth's water is located in seas and ocean and 1.7% of Earth's water is located in the ice caps. Approximately 0.8% is considered to be fresh water. The remaining is made up of brackish water, slightly salty water found as surface water in estuaries and as ground water in salty aquifers(Gleick 1998). Water shortages have plagued many people and human have long searched for a solution to Earth's lack of fresh water supplies.

Today, the world is concern on the problem related to the production of potable water. This is because the project population growth and demand exceed conventional available water resources. According to Service (2006), over one billion people are living without clean drinking water and approximately 2.3 billion people which is 41% of the world population live in region with water shortages. Besides that, most of the solutions that present nowadays are not sufficient to cope with the increasing demand and decreasing supply. Furthermore, most of the traditional source like the river, lake and ground water is misused and causing them to diminish through time (Greenlee et al. 2009). Therefore, as a solution, human being has to find another alternative to overcome this problem. The solution is the seawater because it is abundant and underutilised.

Israel for instance, when their water balance shows an increasing deficit throughout the years and the other regional demands for their water, their authorities has launched the desalination master plan, compromising a large scale seawater desalination of seawater in order to overcome the problem (Lokiec & Kronenberg 2003). While in China, they have been developing seawater technologies for the past six decades to overcome their water shortage problem especially at their coastal areas (Zheng et al. 2014). Thus, desalination is the best solution for the world water shortage problem but it is estimated that some 30% of the world's areas suffer from salinity problem and the remediation is seen very costly (Anon., 2014). Therefore, another method of purifying the seawater need to be developed.

### **1.3 Objectives**

The objectives of this study are:

- a) to synthesize and characterize the hybrid catalyst of titanium dioxide ( $\text{TiO}_2$ ) with biomass ash and metal
- b) to study the effect of the metal loading in photocatalytic seawater purifying processes.

### **1.4 Scope of this research**

The scope of this research are:

- a) Rig set up for the photocatalytic reactor is designed and fabricated.
- b) The catalyst with different weight ratio of  $\text{TiO}_2$  to palm oil fibre ash to metal loading which are Nickel (Ni) or Ferum (Fe) was synthesized using wet impregnation. The catalyst performance was tested in the photocatalytic reactor with the weight ratio of catalyst to seawater of 1:400 for two hours.
- c) Characterization of the fresh and used catalyst using Scanning Electron Microscopy (SEM), Brunauer Emmet Taller(BET) and X-tray Diffraction(XRD) was done.
- d) The pH, conductivity, turbidity, Chemical Oxygen Demand(COD) and Biochemical Oxygen Demand (BOD) were analysed before and after the experiments

## 2 LITERATURE REVIEW

### 2.1 Introduction

Seawater is becoming an increasingly important water source worldwide, and this study aims to examine the effect of metal loading with TiO<sub>2</sub> in the photocatalytic process for seawater purification. An overall aim is to investigate the capability of photocatalytic treatment of saline waters in minimising dissolved organic matter and salt so that it can be used in daily use municipal water.

### 2.2 Photocatalytic process

In 1972, Fujishima and Honda discovered the photocatalytic reaction of water splitting on TiO<sub>2</sub> electrodes. This discovery marked the beginning of a new era in heterogeneous photocatalysis. Since the discovery, there are many research efforts in understanding the fundamental processes and in enhancing the photocatalytic efficiency of TiO<sub>2</sub> have come from extensive research performed by chemists, physicists, and chemical engineers. Such studies are often related to energy renewal and energy storage but in recent years, the heterogeneous photocatalysis has been involved in applications for environmental cleanup. This is inspired by the potential application of TiO<sub>2</sub>-based photocatalysts for the total destruction of organic compounds in polluted air and wastewater (A. Fujishima, 1999).

The current successful photocatalytic systems for overall water splitting can be divided into two primary approaches. The first approach is to split water into H<sub>2</sub> and O<sub>2</sub> using a single visible-light-responsive photocatalyst with a sufficient potential to achieve overall water splitting. In this system, the photocatalyst should have a suitable thermodynamic potential for water splitting, a sufficiently narrow band gap to harvest visible photons, and stability against photocorrosion. Because of these stringent requirements, the number of reliable, reproducible photocatalysts suitable for one-step water splitting is limited (Maeda, et al., 2005; Lee, et al., 2007). The other approach is to apply a two-step excitation mechanism using two different photocatalysts. This approach was inspired by natural photosynthesis in green plants and is called the Z-scheme. The advantages of a Z-scheme water splitting system are that a wider range of visible light is available because a change in Gibbs free energy required to drive each photocatalyst can be reduced as

compared to the one-step water splitting system and that the separation of evolved H<sub>2</sub> and O<sub>2</sub> is possible. It is also possible to use a semiconductor that has either a water reduction or oxidation potential for one side of the system (Bard, 1979).

### **2.3 Photocatalytic Reactor**

Reactor design is an importance focus for photocatalytic reaction because it is importance to perform the experimental work. The reactor design for the photocatalytic reaction can be divided into two categories which are lab scale where the volume of reactant solution is below one litre (Zhang et.al.2011, Natarajan et.al, 2011) and the pilot scale reactor where the reactor volume is more than five litre (Pereira et.al, 2011, Vilar et.al, 2009). The recent innovation for the lab scale reactor are the use of energy efficient UV/visible light emitting diodes (LEDs) as light sources (Wang et.al, 2010, Nickel et.al, 2012), the design of rotating disc type reactor model (Natarajan et.al, 2011, Chang et.al, 2010), the fabrication of NTO-immobilized catalytic beds (Raoet.al, 2012, Ji et.al, 2011) and post-separation/reuse of nano crystalline Titanium Dioxide (NTO) powder catalysts (Kim et.al, 2010, Suryaman et.al, 2012). LEDs are used because the LEDs is a light sources that need less energy and, therefore, LED-based photocatalytic reactors are more energy-efficient systems. The combination of UV-LEDs and NTO powder (Natarajan, 2011), NTO nanotubes , or immobilized NTO (Nickel et.al, 2012) has been reported for the degradation of various dyes such as methyl orange, methylene blue, rhodamine B, and malachite green. The UV-LED photoreactor design by Nickels *et al.* (2012) was equipped with a microcirculating fluid pump so that the reactant is completely mixed and an in-stream sensor unit. The sensor unit, an assembly of a liquid flow cell with transparent windows, an LED lamp, and a photodiode monitor, are installed so that it enabled the real-time evaluation of the decrease in the concentration of methyl orange dye. The reactor also have other special attribute which are it is light weight, low production cost, and flexibility, make this design ideal for both laboratory and field work applications. Visible LEDs with carbon-nitrogen co-doped NTO achieved the visible light degradation of bisphenol (Wang et.al, 2010). The reactor has of four strips of visible LEDs which covered the wavelength range of 450 to 600 nm.

## 2.4 Titanium Dioxide (TiO<sub>2</sub>)

Starting in the late 1960s, researchers study the application and characteristic of TiO<sub>2</sub>. This story, whose keywords are TiO<sub>2</sub> and light, began with photo electrochemical solar energy conversion, and then shifted into the area of environmental photocatalysis and photo-induced hydrophilicity, and most recently into the commercialization of TiO<sub>2</sub>-based photocatalytic products. (Fujishima, 2005)

Titanium dioxide (n-TiO<sub>2</sub>) was recognized to be the most promising semiconductor. It has been widely used as a catalyst because of its optical and electronic properties, low cost, high level of photocatalytic activity, chemical stability and non-toxicity. Over the past several years, the application of TiO<sub>2</sub> as heterogeneous semiconductor has received considerable attention for water splitting to produce hydrogen (Fujishima, 1972; Khan, 1999; Mohaputra, 2007) degradation of organic pollutants (Chen, 1999; Burda, 2003; Magalhães, 2004; Demeestere, et al.,2005; Mohamed, 2005; Park, 2005; Xu, 2006; Chiou, 2008), and wastewater treatment (Oppenlander, 2003; Parsons, 2004). However, owing to its wide band gap (3.0–3.2 eV) titanium n- TiO<sub>2</sub> is a UV absorber. Its photoresponse is limited in the ultraviolet part of the solar spectrum, which is only a small fraction (5%) of the sun's energy.

While, the redox potential for conduction band electrons is –0.52 V, which is negative enough to reduce dioxygen to superoxide, or to hydrogen peroxide. Depending upon the exact conditions, the holes, •OH radicals, O<sub>2</sub><sup>•-</sup>, H<sub>2</sub>O<sub>2</sub> and O<sub>2</sub> itself can all play important roles in the photocatalytic reaction mechanisms (Fujishima, 2005).

## 2.5 Mechanism of Photocatalytic Reaction

The heterogeneous photocatalytic reaction is initiated with the absorption of radiation equal to or higher than the band-gap energy ( $E_{bg}$ ) of the target semiconductor.  $E_{bg}$  is defined as the difference between the filled valence band (VB) and the empty conduction band (CB). When photons with energy equal to or higher than  $E_{bg}$  reach the surface of the photocatalyst, they will cause molecular excitation. As a result, mobile electrons will be generated in the higher-energy CB simultaneously with the generation of positive holes in the lower-energy VB of the photocatalyst. After the initiation of photogenerated electron–hole pairs, the photocatalytic reaction will proceed through a series of chemical events. The photogenerated holes and electrons can either recombine and dissipate the

absorbed energy as heat or be available for use in the redox reaction. Photogenerated holes and electrons that do not recombine migrate to the surface of catalyst for redox reaction. The redox reaction will utilize both the electron and hole, with the positive holes ( $h^+$ ) for oxidation processes and the electrons ( $e^-$ ) for reduction processes on the surface of the photocatalysts. The positive holes break apart the water molecule to form hydron (positive hydrogen cation,  $H^+$ ) and the hydroxyl radical ( $OH^\cdot$ ). This  $OH^\cdot$  will then lead to the production of strong oxidizing  $HO^\cdot$  radicals. Meanwhile, the negative electrons react with the oxygen molecule to form a superoxide anion ( $O_2^{\cdot-}$ ). This superoxide anion also produces  $HO^\cdot$  radicals via the formation of  $HO_2^\cdot$  radicals and  $H_2O_2$ . The electron-hole recombination step is undesirable as it will result in process inefficiencies and waste the energy supplied by the photon. Therefore, it is often considered as one of the major factors limiting the efficiency of the photocatalytic processes (Li Puma et al. 2008). The general mechanism of the photocatalytic reaction on light-illuminated  $TiO_2$  is summarized in Table 2.1.

Table 2-1: General mechanism of the photocatalytic reaction on illuminated  $TiO_2$  (Teh & Mohamed 2011).

| Process  | Reaction steps   |
|--|--|
| Photo-excited $TiO_2$ generates electron-hole pairs ( $h\nu \geq EG$ )   | $TiO_2 \xrightarrow{h\nu} e^- + h^+$   |
| Photogenerated holes, $h^+$ migrate to catalyst surface and react with water molecules adsorbed on the catalyst surface                        | $TiO_2(h^+) + H_2O_{ad} \rightarrow TiO_2 + HO^\cdot + h^+$  |
| $H_2O_{ad}$  |  |
| Photogenerated electrons, $e^-$ migrate to catalyst surface and molecular oxygen acts as an acceptor species in the electron-transfer reaction | $TiO_2(e^-) + O_2 \rightarrow TiO_2 + O_2^{\cdot-}$  |
| Reactions of superoxide anions, $O_2^{\cdot-}$   | $O_2^{\cdot-} + H^+ \rightarrow HO_2^\cdot$ $O_2^{\cdot-} + 3HO_2^\cdot \rightarrow HO^\cdot + 3O_2 + H_2O + e^-$ $2HO_2^\cdot \rightarrow O_2 + H_2O_2$ |

photoconversion of hydrogen peroxide to  $\text{H}_2\text{O}_2 + \text{TiO}_2(\text{e}^-) \rightarrow \text{TiO}_2 + \text{HO}^- + \text{HO} \cdot$   
 give more  $\text{HO} \cdot$  free-radical groups

Oxidization of organic adsorbed pollutants ( $\text{S}_{\text{ad}}$ ) by  $\text{HO} \cdot$  onto the surface of the  $\text{TiO}_2$   
 $\text{HO} \cdot + \text{S}_{\text{ad}} \rightarrow \text{Intermediates}$

Overall reaction  $\text{Organic Pollutant} \rightarrow \text{Intermediates} \rightarrow \text{CO}_2 + \text{H}_2\text{O}$

---

## 2.6 Oil palm fiber ash (Biomass Ash)

Biomass ash are fly ash produce from the combustion of biomass product and it does not contain toxic metal which is found in fly ash from coal combustion. The problem faces from the production of fly ash are the disposal and management of large quantities of fly ash generated because the cost for the disposal is high and have big impact to the environment. Therefore, many researchers are doing research to overcome the problem. The research that has been done for the utilization of the fly ash can be seen in Table 2.2. Fly ash is said to be a promising adsorbent for removal of various pollutants because the adsorption capacity of fly ash may be increased after chemical and physical activation (Ahmaruzzaman 2010). Because of its adsorption capability, a new research will be done on Oil palm fiber ash in purifying the seawater. The biomass ash will be used as a support catalyst for the Titanium Dioxide catalyst. This combination will degrade the contamination present in the seawater.

Table 2-2: The research on utilization of fly ash.

| Title   | Researcher        |
|---|-------------------|
| Use Of Coal Fly Ash As A Catalyst In The Production of Biodiesel  | (Ameer 2010)      |
| Synthesis of Nanocrystalline $\text{TiO}_2$ -Coated Coal Fly Ash For Photocatalyst  | (Yu 2003)         |
| Favorable Recycling Photocatalyst $\text{TiO}_2$ /CFA: Effects of Loading Method on The Structural Property And Photocatalytic Activity | (Shi et al. 2009) |

---

## 2.7 Metal Loading in Photocatalyst

Titanium dioxide is one of the most efficient photocatalysts for the detoxication of organically charged waste water but this material suffers from the drawback of poor absorption properties because of a band gap of 3.2 eV. The wavelengths of Titanium Dioxide is shorter than 400 nm which are needed for light induced generation of electron±hole pairs. Therefore, many researcher are trying to overcome the band gap problem. One of the way to overcome this problem is doping with transition metal ions for inducing a batho-chromic shift of the band gap. However, this doping changes other physical properties such as lifetime of electron±hole pairs and adsorption characteristics (Wilke & Breuer 1999). The research involving the band gap can be seen in Table 2.3. For this paper, the metal that will be used are Ferum and Nickel. This metal will be mix with Titanium Dioxide and biomass ash with different weight ratio. This mixture will increase the band gap so that the reaction can be done using sunlight and improve the quality of the seawater.

Table 2-3: The research on effect of metal in photocatalyst.

| <b>Title</b>  | <b>Researcher</b>         |
|---|---------------------------|
| Bandgap studies on anatase titanium dioxide nanoparticles   | (Reddy et al. 2002)       |
| Role of Fe Doping in Tuning the Band Gap of TiO <sub>2</sub> for the Photo-Oxidation-Induced Cytotoxicity Paradigm                                | (George et al. 2011)      |
| Preparation and Characterization of Fe <sup>3+</sup> , La <sup>3+</sup> Co-Doped Tio <sub>2</sub> Nanofibers and Its Photocatalytic Activity      | (Wu et al. n.d.)          |
| Semiconductor-Metal Composite Nanostructures. To What Extent Do Metal Nanoparticles Improve the Photocatalytic Activity of TiO <sub>2</sub> Films | (Subramanian et al. 2001) |

### 3 MATERIALS AND METHODS

#### 3.1 Introduction

For this chapter, there is an explanation of the material used and detailed procedure that were used to run this experiment to achieve the objective of this research. Summarization of the experimental flow chart related to experimental procedure is shown in Figure 3-1.

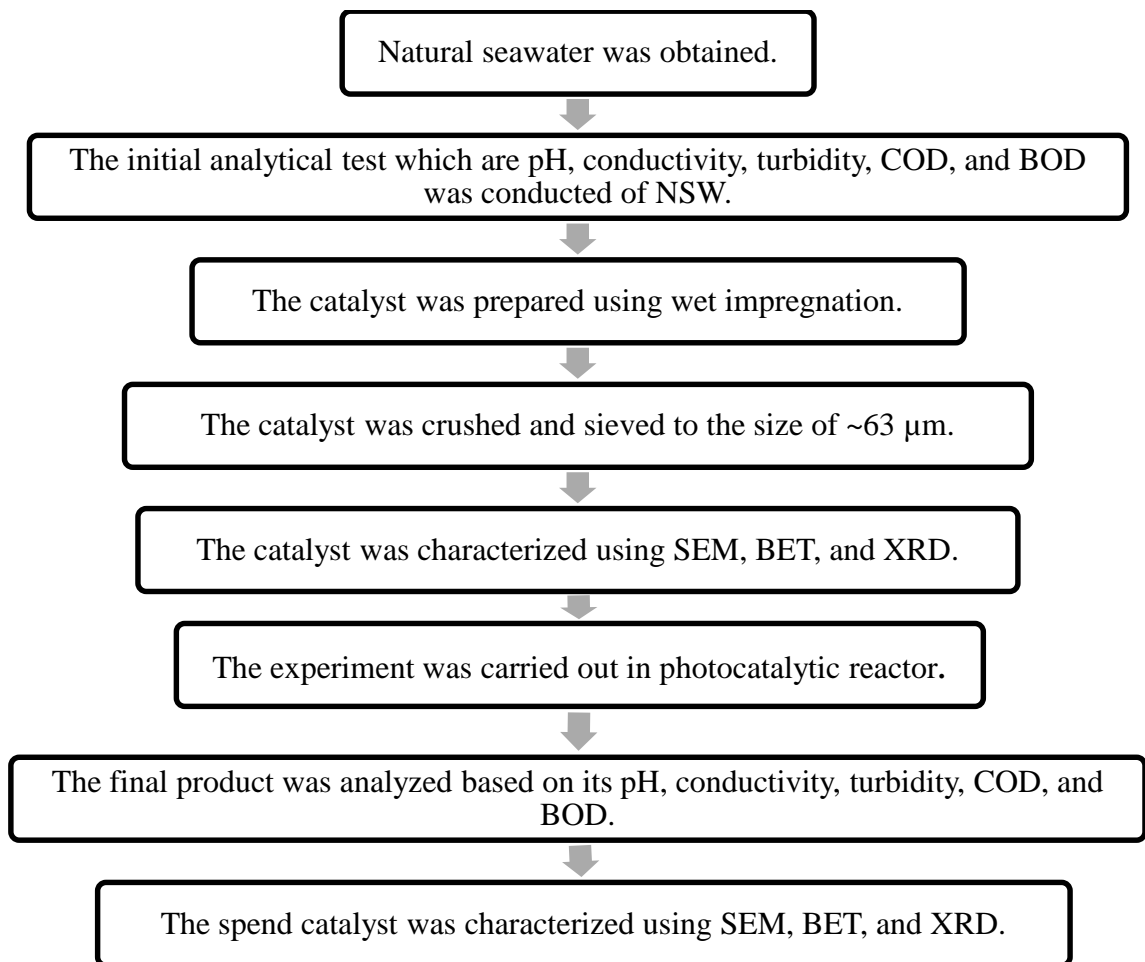


Figure 3-1: Flow diagram of experimental procedure.

## **3.2 Material**

For this research, the raw materials used for photocatalytic reaction preparation were natural seawater (NSW) and palm oil fibre ash (Biomass ash). While the chemicals used for these research were Titanium Dioxide ( $\text{TiO}_2$ ) catalyst, Nickel Nitrate Hexahydrate ( $\text{Ni}(\text{NO}_3)_2 \cdot 6\text{H}_2\text{O}$ ), and Ferum (III) Nitrate nonaydrate ( $\text{Fe}(\text{NO}_3)_3 \cdot 9\text{H}_2\text{O}$ ).

### **3.2.1 Natural Seawater (NSW)**

The NSW sample from Teluk Cempedak Kuantan, Pahang. The sample was stored at 4 °C in the refrigerator.

### **3.2.2 Oil palm fiber ash (Biomass ash)**

Oil palm fiber ash was obtained from Felda Lepar Hilir 3 palm oil mill, Gambang, Kuantan, Pahang. It was used as a catalays supporter for  $\text{TiO}_2$ .

### **3.2.3 Chemical**

The chemical used was  $\text{TiO}_2$  powder with 99% purity, Nickel Nitrate Hexahydrate ( $\text{Ni}(\text{NO}_3)_2 \cdot 6\text{H}_2\text{O}$ ) with 99% purity, Iron(III) Nitrate Nonahydrate ( $\text{Fe}(\text{NO}_3)_3 \cdot 9\text{H}_2\text{O}$ ) with 99% purity. These three chemical was obtained from Sigma-Aldrich Malaysia.

## **3.3 Preparation of Solution and Catalyst**

### **3.3.1 Preparation of NSW**

For the natural seawater, the seawater was obtained from Teluk Cempedak, Kuantan, Pahang. The NSW was stored in a refrigerator at 4 °C. The volume of the NSW used for each experiment was depend on the weight ratio of 1:400 which represent the weight of catalyst and the weight of the NSW respectively.

### 3.3.2 Preparation of Catalyst

For this research, three type of catalyst were produced via wet impregnation. The detail of the catalyst is illustrated in Table 3-1. The solution was stirred by using hot plate at 80°C for four hours. The solution was then dried overnight at 100°C in the oven. After that, the solution was calcined at 500°C for four hours in the furnace. The solution was then crushed and sieved to the size of ~63µm.

Table 3-1: The weight ratio of the three catalyst.

| Catalyst         | Weight Ratio (%) |             |                     |
|------------------|------------------|-------------|---------------------|
|                  | TiO <sub>2</sub> | Biomass Ash | Metal(Nickel/Ferum) |
| No metal loading | 50               | 50          | 0                   |
| Nickel loading   | 45               | 45          | 10                  |
| Ferum loading    | 45               | 45          | 10                  |

### 3.3.3 Characterization of Catalyst

The fresh and used catalyst were characterized by using X-ray Diffraction (XRD), Scanning Electron Microscopy (SEM) and Brunauer Emmett Teller (BET). The catalyst was characterized by using XRD to determine the crystal structure of the catalyst. While SEM was used to determine the catalyst's surface mophology. BET surface analysis was used to measure the total specific surface area, pore size and pore volume of the catalyst.

#### 3.3.3.1 Scanning Electron Microscopy (SEM)

SEM (CAEL ZEISS) was used for catalyst characterization and surface morphology analysis. A high resolution SEM coupled to an energy dispersive X-tray spectrometer system was producing various signals contained the information regarding the sample's surface topography and composition. Then the samples were mounted on a stub of metal with adhesive, coated with 40 - 60 nm of metal such as Gold/Palladium and then were observed in the microscope.



Figure 3-2: Scanning Electron Microscopy (SEM).

### 3.3.3.2 Brunauer Emmett Teller (BET)

BET (Micromeritics ASAP2020) surface analysis was used for measuring the total specific area, pore size, and pore volume of the catalysts. This instrument provide precise evaluation of material by nitrogen multilayer adsorption measured as a function of relative pressure using fully automated analyzer. The samples were degassed in a vacuum at high temperatures. The highest temperature possible that will not damage the sample's structure is usually chosen in order to shorten the degassing time. IUPAC recommends that samples be degassed for at least 16 hours to ensure that unwanted vapors and gases are removed from the surface of the sample. About of 0.5 g of sample was required for the BET to successfully determine the surface area. Then the samples were placed in glass cells to be degassed at 200 °C for six hours and then analyzed by the BET machine.



Figure 3-3: Brunauer Emmett Teller (BET).

### 3.3.3.3 X-ray Diffraction (XRD)

XRD (ADX-2500) was used to determine the composition of the catalyst. The XRD technique takes a sample of the material and places a powdered sample on a holder, then the sample was illuminated with x-rays of a fixed wave length and the intensity of the reflected radiation was recorded using goniometer. The data then analysed for the reflection angle to calculate the inter atomic spacing.



Figure 3-4: X-Ray Diffraction (XRD).

### 3.4 Photocatalytic Reactor Set Up

The photocatalytic reactor (Figure 3-5) with a diameter of eight centimeters and height of 30 cm was set up consisting of black box, cooling fan, temperature controller, reactor, hot plate, magnetic stirrer, silicon tubing and mercury light. The mercury light was placed beside the reactor at distance at three centimeter. The experiment was run inside the black box to prevent the UV light exposure to the surrounding environment.

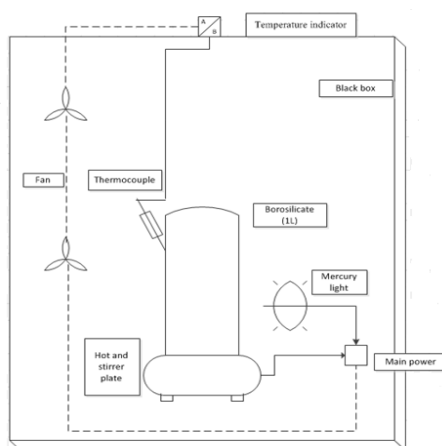


Figure 3-5: The schematic diagram of photocatalytic reactor